Report on:

Key differences between the IROE-R processor and the IROE processor improved in the frame of the AMIL2DA study

Version: Issue 1 (DRAFT)

Delivery D42 of WP 4500 of the study:

"Advanced MIPAS Level 2 Data Analysis (AMIL2DA)"

Project: **EVG1-CT-1999-00015**

Prepared by:

S. Ceccherini	IFAC – CNR (formerly IROE – CNR), Firenze (Italy)
M. Ridolfi	University of Bologna (Italy)

14 March 2002

CONTENTS

1. Introduction

Starting from 1995, in the frame of an ESA supported study involving a large international consortium of scientists, IROE developed an Optimized Forward Model (OFM) and an Optimized Retrieval Model (ORM) suitable for implementation in the ESA ground processing chain taking care of Near Real Time (NRT) Level 2 retrievals from MIPAS spectra. The OFM is a self-standing forward model with the capability of simulating synthetic observations to be employed mainly for testing the ORM algorithm. The inversion algorithm of the ORM contains an internal function with the capability of generating spectra identical to the ones generated by the OFM. Due to the very stringent runtime requirements for the NRT algorithm, several optimizations and approximations were implemented in the OFM and the ORM processors. The impact of the individual approximations on retrieval accuracy was checked during the development of the codes by means of both self-consistency tests and intercomparisons against a Reference Forward Model (RFM) developed at Oxford University and optimized for accuracy performance. Despite this conservative approach adopted for the development of the OFM and ORM codes, the effect of possible systematic differences between observations and simulations (due to systematic errors in the forward model internal to the retrieval scheme) on the retrieval behaviour was mostly unknown before the tests carried-out under the AMIL2DA study.

The OFM and ORM codes developed at IROE for the ESA NRT processor of MIPAS will be indicated as OFM_R and ORM_R respectively (_R = reference). The algorithms implemented in these processors are described in *Ridolfi et al. (2000)*.

The forward model intercomparison exercise carried-out in the present study (WP 3000) highlighted some deficiencies of the OFM_R algorithm. In particular it was shown that the following spectroscopic effects neglected in the OFM_R may significantly affect the accuracy of the simulated spectra in localized spectral / altitude regions and in particular atmospheric conditions:

1. Pressure-shift
2. Self-broadening
3. Line-mixing
4. Non Local Thermal Equilibrium (NLTE)

We therefore improved the OFM_R and generated an OFM_I (_I = improved) that includes the effects 1, 2 and 3 in the forward calculations. NLTE was not implemented in the OFM_I because its implementation would have required a complete re-design of the code and dropping of several of the most effective runtime optimizations currently implemented in the code. Finally, compared to the OFM_R, the OFM_I includes an upgraded model for H_2O continuum (CKD 2.4 vs. CKD 2.1).

The OFM_I is a useful tool that can be employed to generate high-accuracy spectra supporting the interpretation of the residuals of the fit of real spectra. So far the OFM_I was extensively used in the analysis of the discrepancies between the OFM_R and the other forward models considered in the AMIL2DA study.

Even if in general the accuracy of the forward model turns-out to be improved when considering the above effects 1, 2 and 3, it should be noted that effects 1 and 2 have usually little impact on MIPAS spectra simulated under realistic atmospheric conditions (self broadening might be important only at very low altitudes for water lines) and effect 3. (line-mixing), as simulated in the OFM_I, impacts only localized spectral regions (Q-branches of CO_2).

For this reason we decided not to upgrade the forward model internal to the retrieval scheme (ORM_R) and to avoid the above effects (1, 2, 3 and 4) by adopting an appropriate selection of spectral intervals (microwindows) for the retrieval. The microwindows are selected using an optimization scheme developed at Oxford University and described in *Dudhia (1999)*. This approach allows also for an accurate estimation of the various error components affecting the retrieved profiles.

This is also the approach used in ESA's near real-time Level 2 processor. The performances of the

ORM_R as resulting from the blind test retrievals carried-out as part of WP 4000 are described in Sect. 3 of the present document.
If on one hand the joint exploitation of the optimized microwindow selection scheme and the ORM_R algorithm is expected to provide sufficient accuracy with respect to the neglected effects 1, 2, 3 and 4, on the other hand there is a general concern regarding some instrument-related quantities derived in Level 1b processing and assumed as known in the Level 2 chain. In particular the following quantities determined in the Level 1b processor

- ILS shape
- Frequency calibration
- Intensity calibration
- Instrumental offset

could be affected by a significant error with consequent impact on Level 2 retrieval performance. For this reason we decided to upgrade the ORM_R algorithm in order to allow for a quantification and possibly for a correction of the errors associated with the above quantities. The "improved" version of the ORM_R is named ORM_I (_I = improved) that, compared to the ORM_R, has the additional flexibility that the user can define via input files the retrieval vector. In addition to the usual state parameters retrieved by the ORM_R, it is also possible to (optionally) retrieve from measured spectra the following parameters:

- ILS broadening parameter (one parameter / spectral band)
- Frequency scaling parameter (one parameter / spectral band)
- Intensity scaling parameter (one parameter / spectral band)
- MW- and altitude- dependent instrumental offset (ORM_R is able to fit only a MW-dependent instrumental offset).

Of course the ORM_I can also be operated with the same state vector defined in the ORM_R and in this case it produces the same results of the ORM_R.
In Sect. 4 of the present document we describe the new functionalities implemented in the ORM_I. In Sect. 5 we show the results of tests carried-out with the aim of characterizing the feasibility of the retrieval of the new parameters considered in the ORM_I.

2. Scope of the document

Scope of the present document is:

a) to summarize the performance of the ORM_R resulting from the blind test-retrievals carried-out under WP 3000 (of the AMIL2DA study)
b) to describe the new functionalities implemented in the ORM_I
c) to define the limits of applicability of the new options implemented in the ORM_I.

3. Performances of the ORM_R resulting from blind test retrievals

For the blind test retrievals exercise IAA generated MIPAS simulated observations using the KOPRA forward model with unknown atmosphere and conservative processing setup parameters. Starting from these observations the retrieval of pT and of the six MIPAS high-priority species (H_2O, O_3, HNO_3, CH_4, N_2O and NO_2) was carried-out using the ORM_R with spectral microwindows selected by the Oxford University tool (*Bennett et al., (1999)*) on July 2001. The spectral intervals used in the retrievals presented in this section are reported in Table 1.
In particular, two different sets of simulated observations were generated by IAA and therefore two different sets of retrievals were carried-out:

- BTS1 retrievals. Temperature (T) and instrument pointing angles are known (supplied by IAA). Therefore only retrievals of VMRs of the MIPAS key species were undertaken in this case.
- BTS2 retrievals. T, pointing angles and VMRs are all unknown. Therefore in this case we first

simultaneously retrieve T and tangent pressure (pointing) and then VMRs of the six key species sequentially, using previously retrieved p, T (and VMRs, if any).

Figures from 1 to 6 show the results of BTS1 retrievals while figures from 7 to 14 show the results of BTS2 retrievals. In each of the figures 1-14 we show:

(a) left panels: retrieved (solid line with error bars), reference (dashed line) and initial guess (dotted line) profiles

(b) right panels: percentage differences between retrieved and reference (true) profiles (open symbols), strip of ± total error (solid line) as resulting from the quadratic summation of the random error evaluated from the retrieval covariance matrix (VCM) and the systematic component as estimated by the microwindow selection tool (MWMAKE) developed at Oxford University (*Bennett et al., (1999)*).

In the right panels we also show the value of the χ^2 of the profile evaluated as:

$$\chi^2 = \frac{1}{N_{RET}} \sum_{j=1}^{N_{RET}} \frac{\left(x_{RET}(j) - x_{REF}(j)\right)^2}{\sigma_{TOT}^2(j)} \qquad (1)$$

where:

N_{RET} = number of retrieved points in the profile

$x_{RET}(j), x_{REF}(j)$ = retrieved and reference (respectively) values of the *j-th* parameter

$\sigma_{TOT}(j)$ = total error relating to the *j-th* retrieved parameter

Please note that (1) is just a quantifier for the discrepancies between retrieved and true profiles, it is not the χ^2-test of the retrieval.

General remarks:

- The microwindows (Version JUL01) used for the test retrievals reported in the present document do not coincide with those that are planned to be used by the ESA on-line Level 2 processor during the commissioning phase. During this phase ESA's on-line Level 2 processor will use a slightly different set of microwindows (Version DEC01) that, compared to the JUL01 version, is less demanding in terms of computing time but, of course, provides less accurate results.
- All tests presented in this document have been run using a constraint on the retrieved continuum parameters. In particular, the atmospheric continuum is assumed to vary linearly with frequency within spectral intervals of 10 cm^{-1}. Rigorously speaking, this constraint is not consistent with the most recent versions of the Oxford MW selection algorithm that assumes the fitted continuum parameters to be uncorrelated in the frequency domain (the fitted continuum parameters are exploited to compensate for systematic errors that may not vary smoothly as a function of frequency). However we repeated both BTS1 and BTS2 retrievals also without this continuum constraint and found that, in this particular case, the results are not affected at all by the constraint. We must however keep in mind that this constraint should not be used when retrievals are operated on real spectra.
- All tests presented in this document have been run using cross-section lookup-tables (LUTs) and irregular spectral grids (see *Ridolfi et al., (2000)*) calculated by the Oxford University team. The used LUTs have been generated including pressure-shift and self-broadening effects. However, we also made a test in which all retrievals were repeated using line-by-line (LBL) calculation of cross-sections and we found that differences between profiles retrieved with LUTs and LBL are well below the random retrieval error.

PT retrieval			
1	PT___oxf_039	685.7000	685.8250
2	PT___oxf_001	686.4000	689.4000
3	PT___oxf_017	696.2000	698.3750
4	PT___oxf_037	694.8000	695.1000
5	PT___oxf_038	700.4750	701.0000
6	PT___oxf_004	728.3000	729.1250
7	PT___oxf_026	1349.4000	1350.8750
8	PT___oxf_022	1353.3250	1354.8250
9	PT___oxf_034	1357.2000	1358.0000
10	PT___oxf_021	1932.8500	1934.3500
H2O retrieval			
1	H2O__oxf_002	807.8500	808.4500
2	H2O__oxf_027	1374.1250	1375.0750
3	H2O__oxf_026	1394.4750	1395.7750
4	H2O__oxf_021	1454.5250	1457.5250
5	H2O__oxf_011	1574.8000	1577.8000
6	H2O__oxf_001	1650.0250	1653.0250
O3 retrieval			
1	O3___oxf_021	763.3750	766.3750
2	O3___oxf_012	1073.8000	1076.8000
3	O3___oxf_001	1122.8000	1125.8000
HNO3 retrieval			
1	HNO3_oxf_001	876.3750	879.3750
2	HNO3_oxf_006	885.1000	888.1000
3	HNO3_oxf_012	895.6750	898.6750
4	HNO3_oxf_021	1319.0500	1322.0500
5	HNO3_oxf_003	1324.1750	1327.1750
CH4 retrieval			
1	CH4__oxf_012	1227.1750	1230.1750
2	CH4__oxf_013	1247.7750	1248.6500
3	CH4__oxf_005	1256.6750	1257.6500
4	CH4__oxf_001	1350.8750	1353.8750
5	CH4__oxf_022	1607.7500	1610.7500
N2O retrieval			
1	N2O__oxf_021	1161.6250	1164.6250
2	N2O__oxf_012	1233.2750	1236.2750
3	N2O__oxf_004	1256.6750	1257.9750
4	N2O__oxf_005	1262.3500	1263.1250
5	N2O__oxf_008	1265.7500	1266.8000
6	N2O__oxf_001	1272.0500	1275.0500
NO2 retrieval			
1	NO2__oxf_001	1607.2750	1610.2750
2	NO2__oxf_003	1613.7250	1616.6000
3	NO2__oxf_010	1619.1250	1622.1250
4	NO2__oxf_013	1622.5500	1623.4750
5	NO2__oxf_006	1624.8000	1627.8000

Table 1: microwindows used for blind test retrievals.

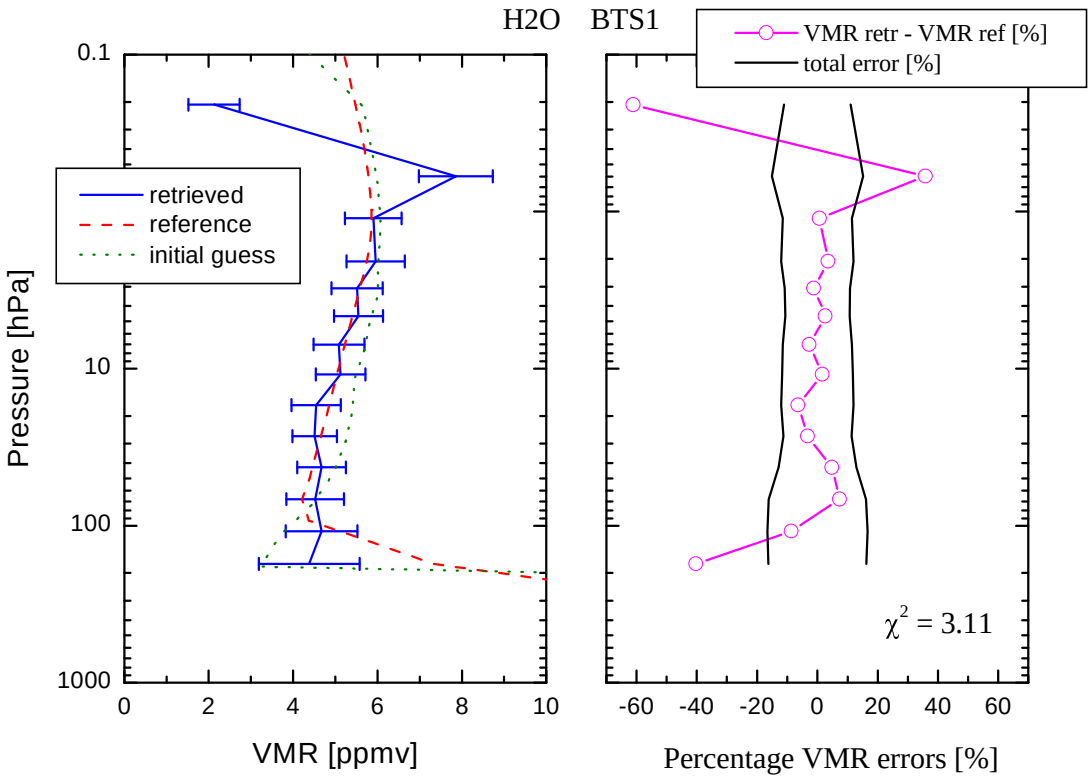
H2O BTS1
VMR retr - VMR ref [%]
total error [%]
retrieved
reference
initial guess
Pressure [hPa]
0.1
10
100
1000
0
2
4
6
8
10
VMR [ppmv]
-60
-40
-20
0
20
40
60
Percentage VMR errors [%]
χ² = 3.11

Fig. 1

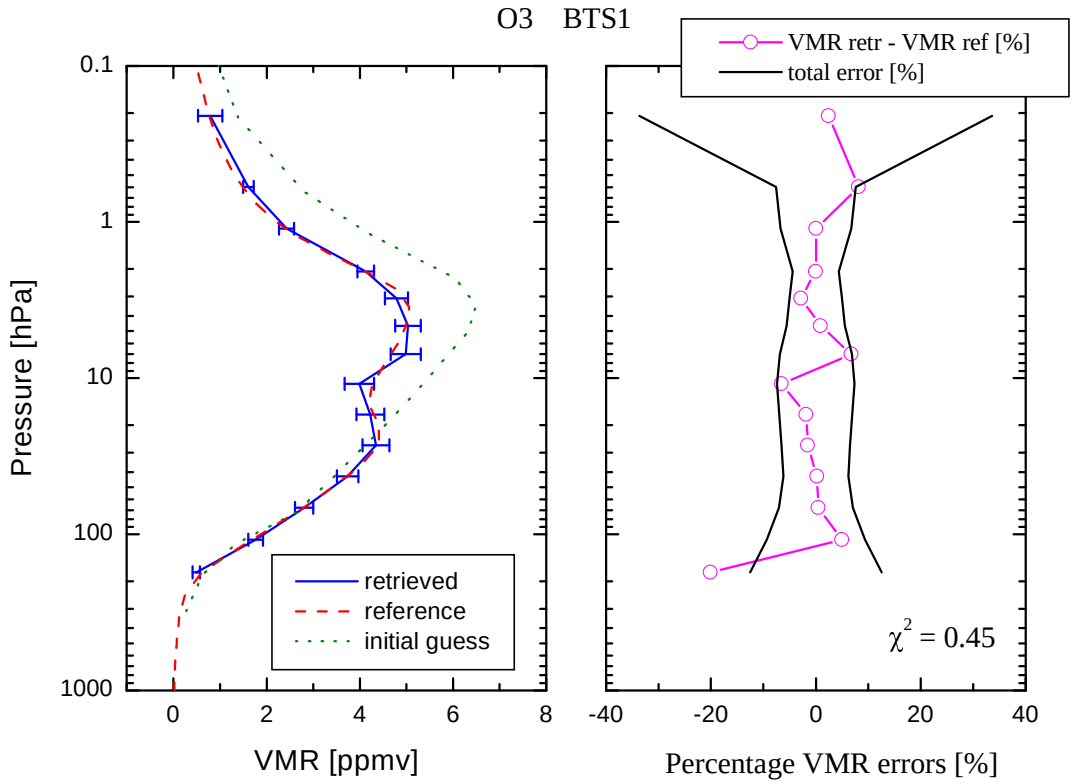
O3 BTS1
VMR retr - VMR ref [%]
total error [%]
retrieved
reference
initial guess
Pressure [hPa]
0.1
1
10
100
1000
0
2
4
6
8
VMR [ppmv]
-40
-20
0
20
40
Percentage VMR errors [%]
χ² = 0.45

Fig. 2

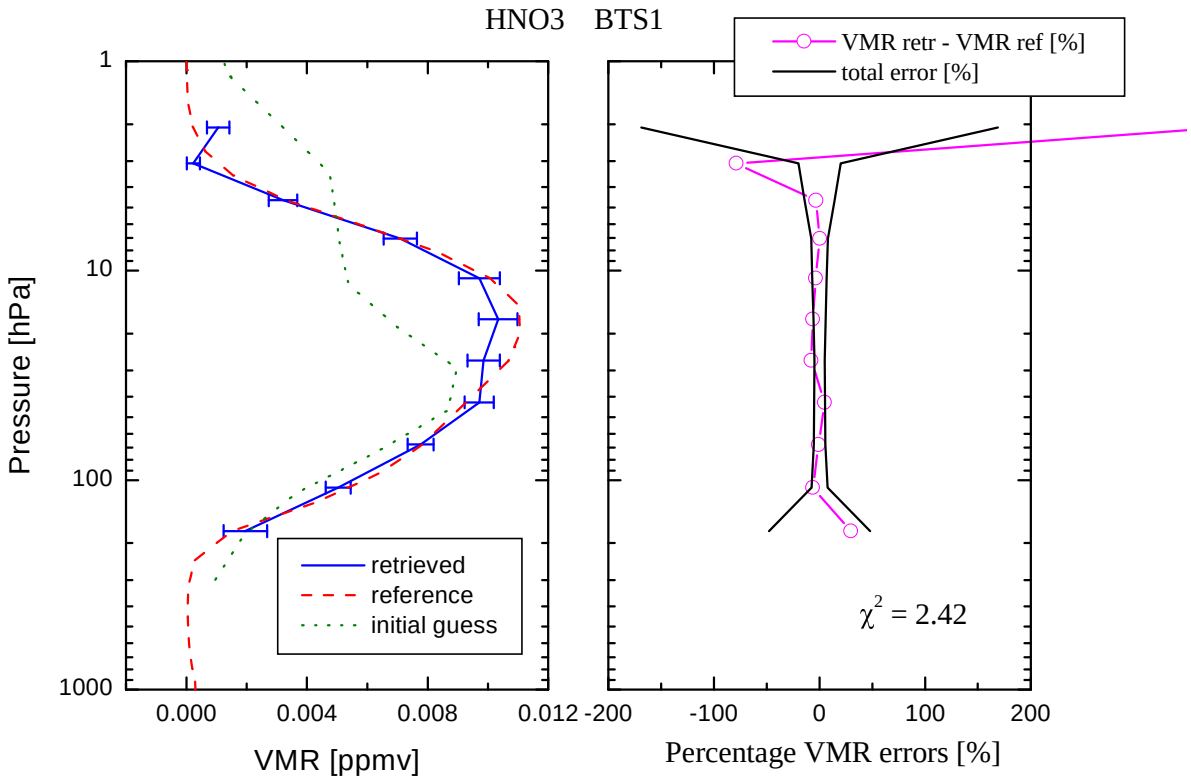
HNO3 BTS1
VMR retr - VMR ref [%]
total error [%]
Pressure [hPa]
1
10
100
1000
retrieved
reference
initial guess
0.000
0.004
0.008
0.012
VMR [ppmv]
-200
-100
0
100
200
Percentage VMR errors [%]
χ² = 2.42

Fig. 3

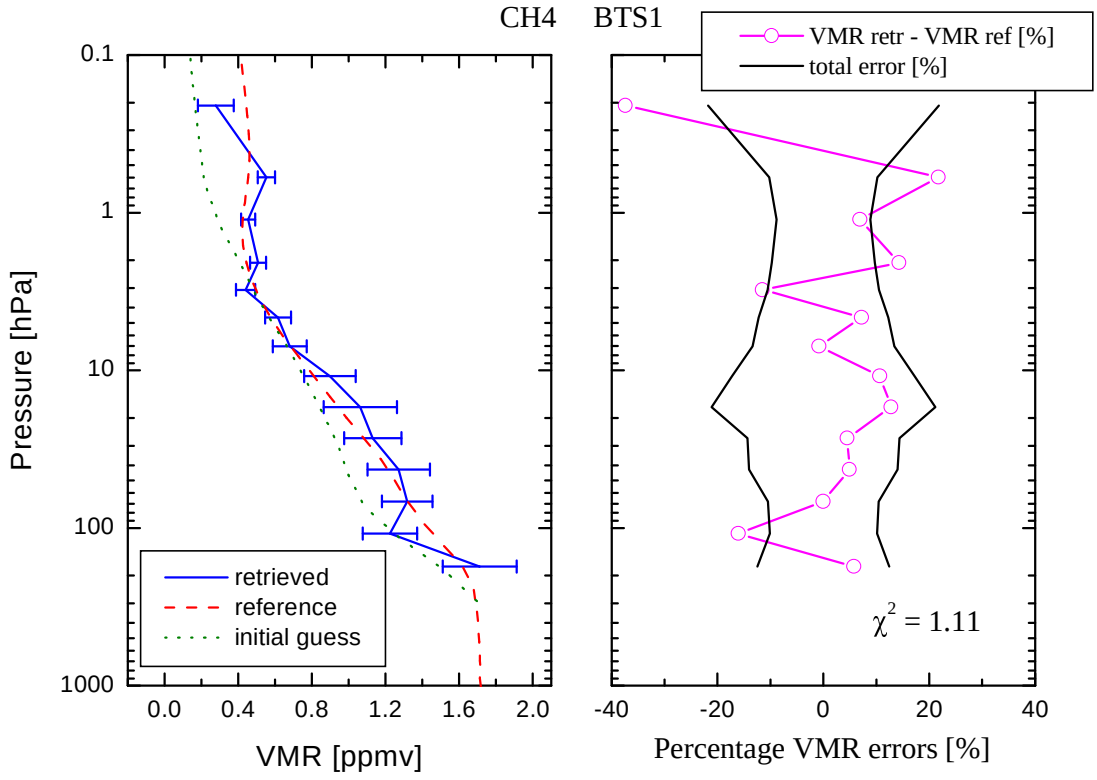
CH4 BTS1
VMR retr - VMR ref [%]
total error [%]
Pressure [hPa]
0.1
1
10
100
1000
retrieved
reference
initial guess
0.0
0.4
0.8
1.2
1.6
2.0
VMR [ppmv]
-40
-20
0
20
40
Percentage VMR errors [%]
χ² = 1.11

Fig. 4

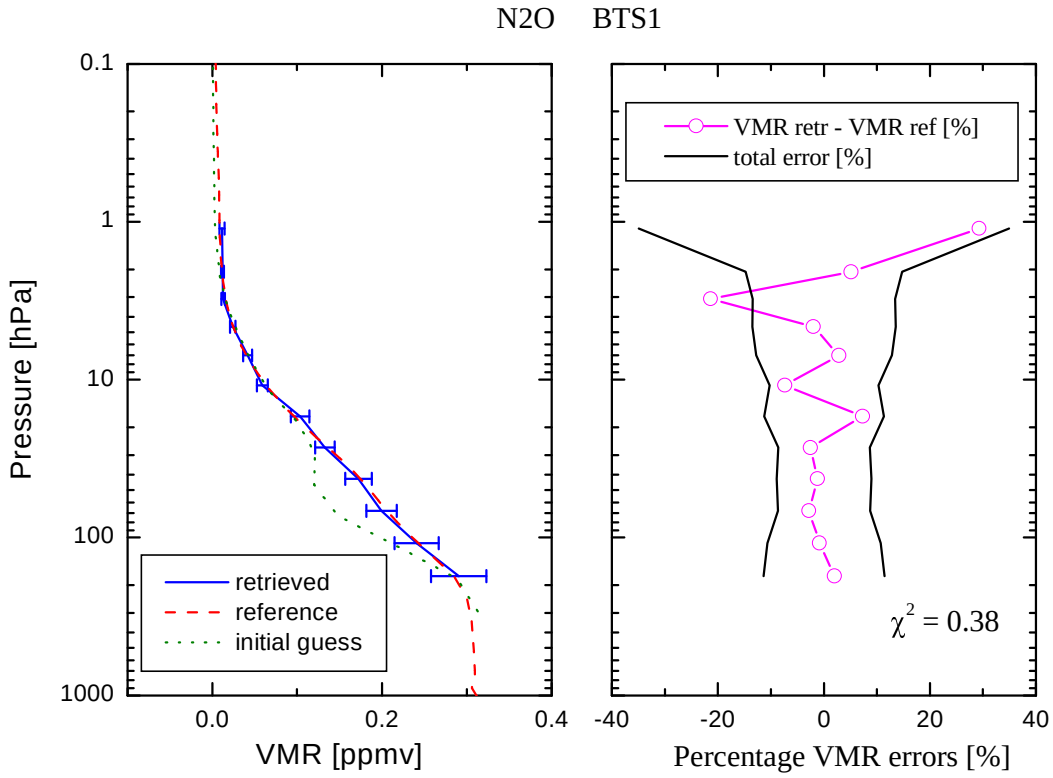
N2O BTS1
Pressure [hPa]
0.1
1
10
100
1000
0.0
0.2
0.4
VMR [ppmv]
retrieved
reference
initial guess
VMR retr - VMR ref [%]
total error [%]
χ^2 = 0.38
-40
-20
0
20
40
Percentage VMR errors [%]

Fig. 5

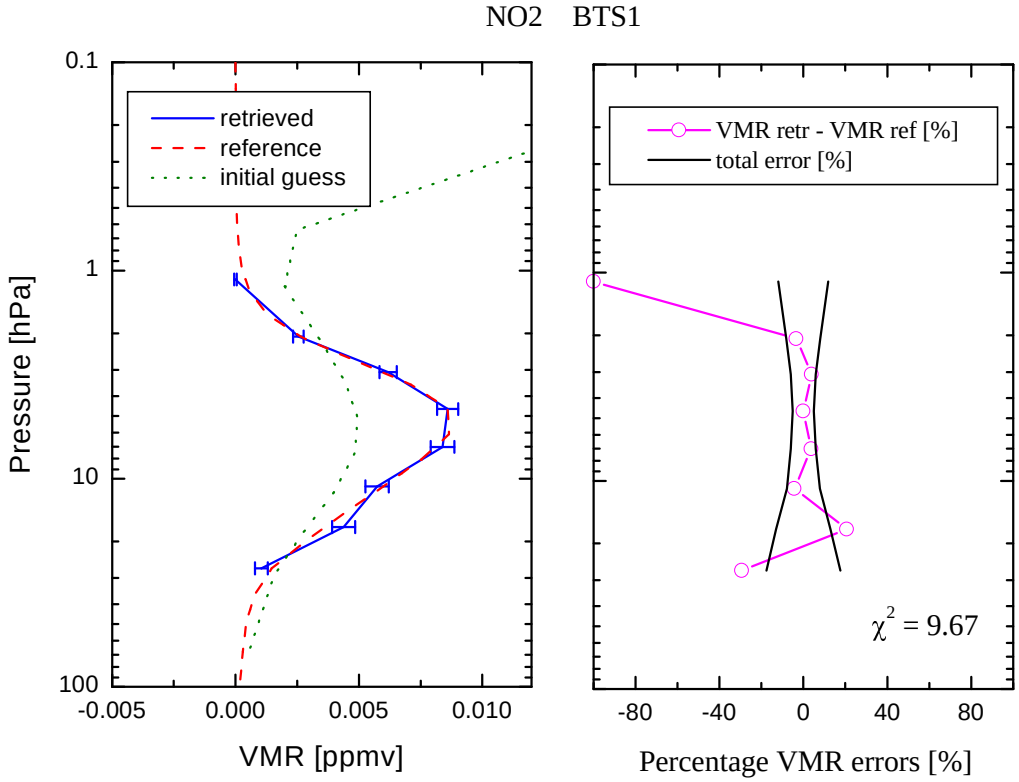
NO2 BTS1
Pressure [hPa]
0.1
1
10
100
-0.005
0.000
0.005
0.010
VMR [ppmv]
retrieved
reference
initial guess
VMR retr - VMR ref [%]
total error [%]
χ^2 = 9.67
-80
-40
0
40
80
Percentage VMR errors [%]

Fig. 6

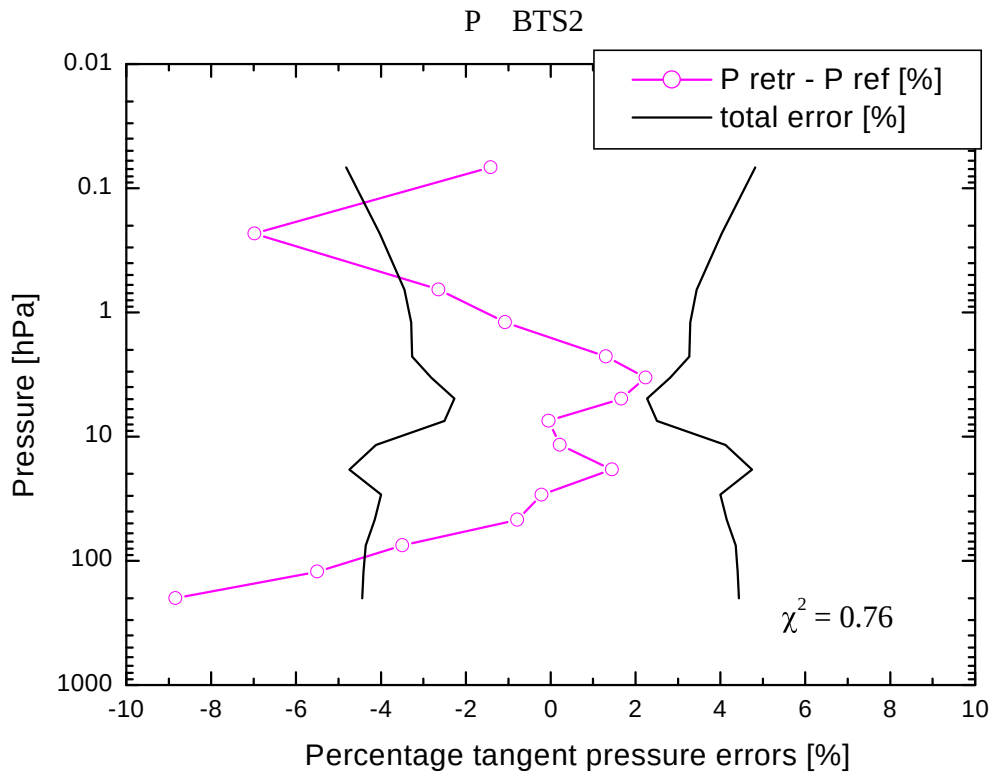
P BTS2
P retr - P ref [%]
total error [%]
Pressure [hPa]
0.01
0.1
1
10
100
1000
-10
-8
-6
-4
-2
0
2
4
6
8
10
Percentage tangent pressure errors [%]
χ² = 0.76

Fig. 7

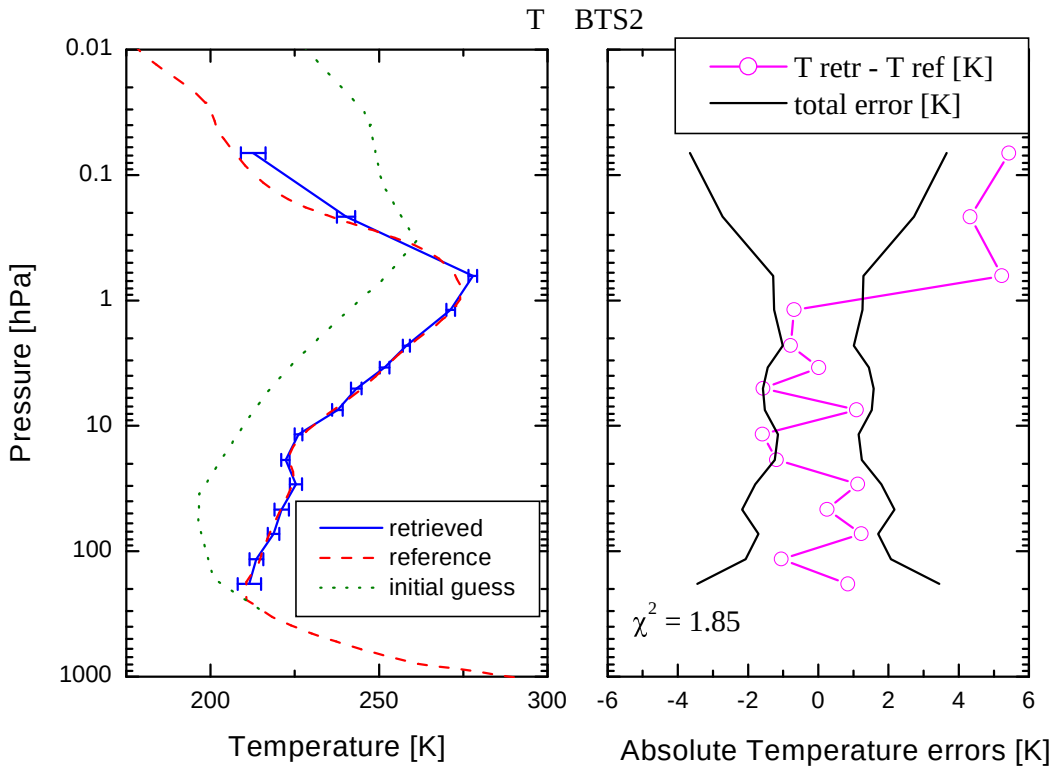
T BTS2
T retr - T ref [K]
total error [K]
retrieved
reference
initial guess
Pressure [hPa]
0.01
0.1
1
10
100
1000
200
250
300
Temperature [K]
-6
-4
-2
0
2
4
6
Absolute Temperature errors [K]
χ² = 1.85

Fig. 8

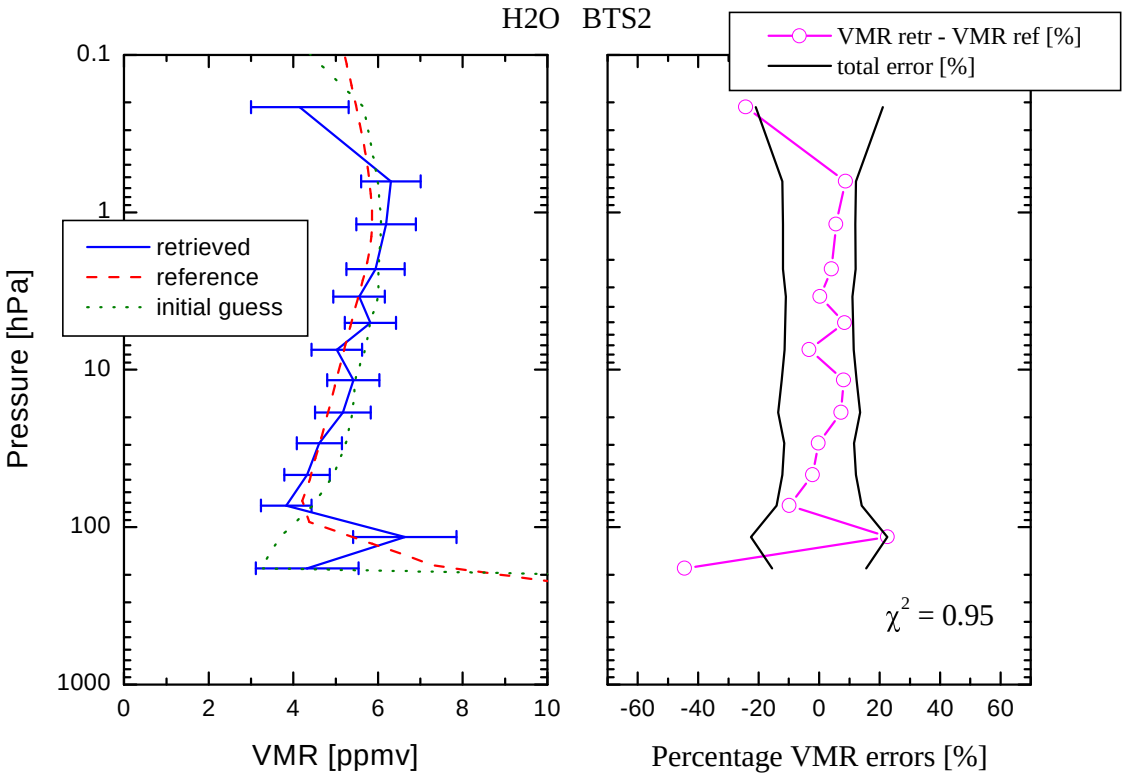
H2O BTS2
VMR retr - VMR ref [%]
total error [%]
retrieved
reference
initial guess
Pressure [hPa]
0.1
1
10
100
1000
0
2
4
6
8
10
VMR [ppmv]
-60
-40
-20
0
20
40
60
Percentage VMR errors [%]
χ^2 = 0.95

Fig. 9

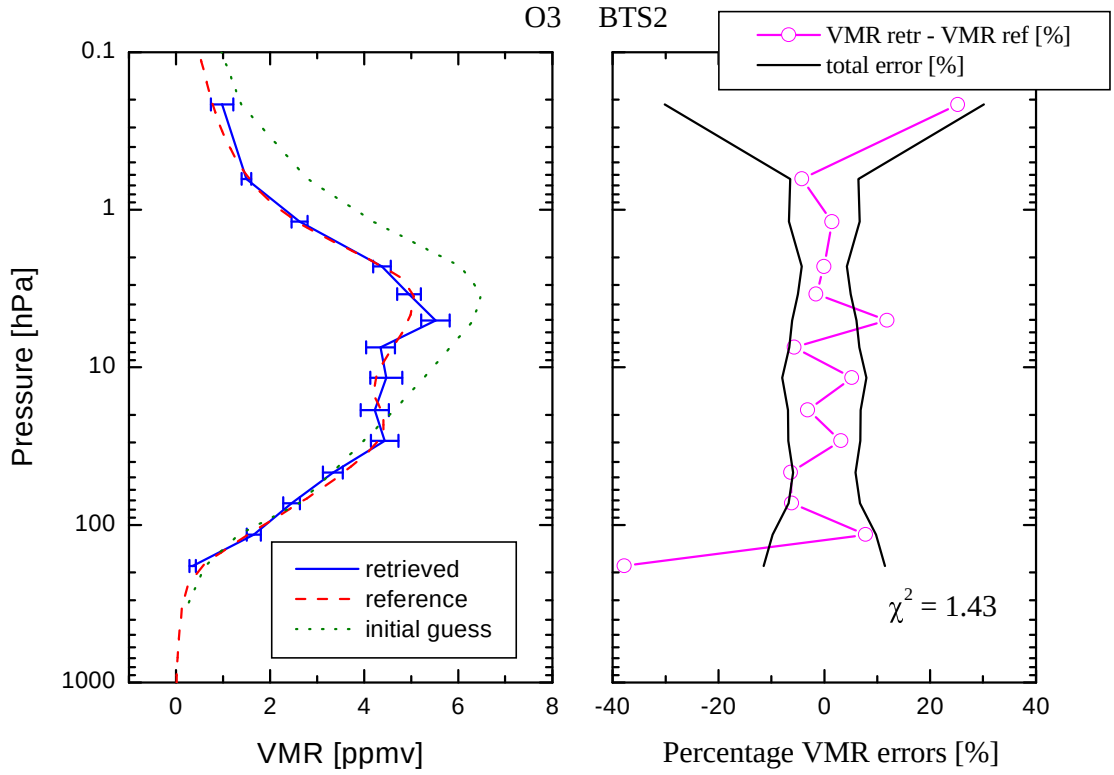
O3 BTS2
VMR retr - VMR ref [%]
total error [%]
retrieved
reference
initial guess
Pressure [hPa]
0.1
1
10
100
1000
0
2
4
6
8
VMR [ppmv]
-40
-20
0
20
40
Percentage VMR errors [%]
χ^2 = 1.43

Fig. 10

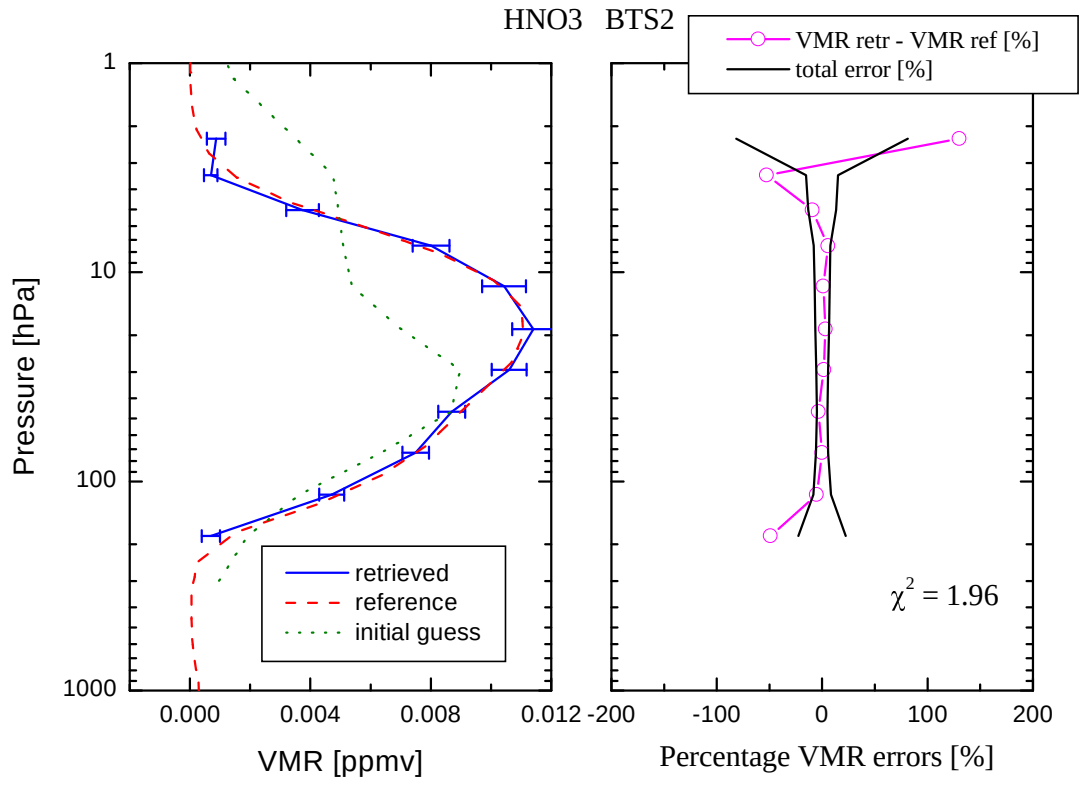
HNO3 BTS2
VMR retr - VMR ref [%]
total error [%]
Pressure [hPa]
1
10
100
1000
retrieved
reference
initial guess
0.000
0.004
0.008
0.012
VMR [ppmv]
-200
-100
0
100
200
Percentage VMR errors [%]
χ² = 1.96

Fig. 11

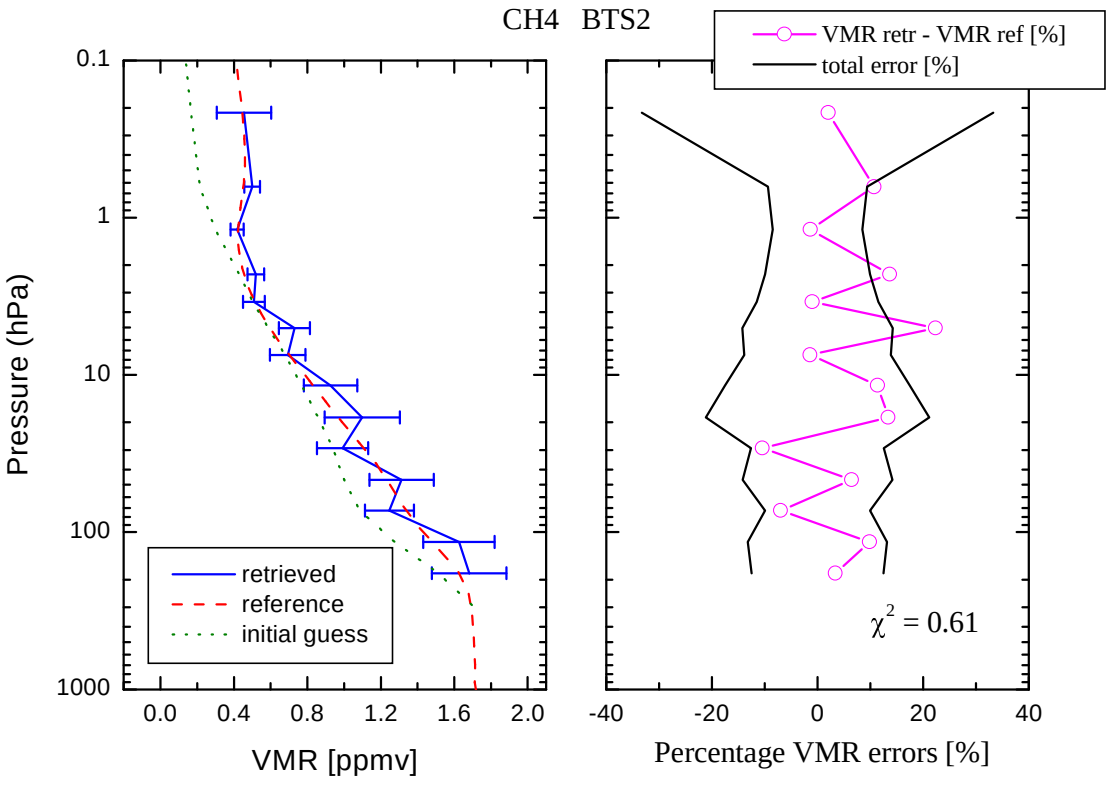
CH4 BTS2
VMR retr - VMR ref [%]
total error [%]
Pressure (hPa)
0.1
1
10
100
1000
retrieved
reference
initial guess
0.0
0.4
0.8
1.2
1.6
2.0
VMR [ppmv]
-40
-20
0
20
40
Percentage VMR errors [%]
χ² = 0.61

Fig. 12

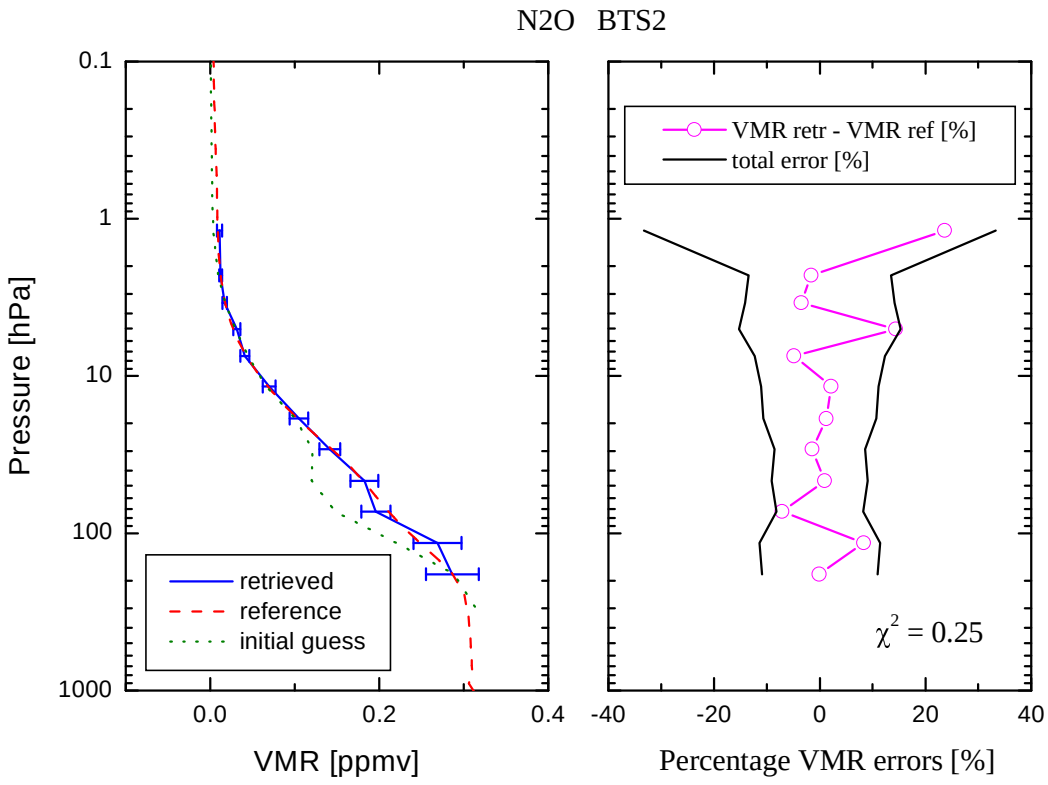
N2O BTS2
Pressure [hPa]
0.1
1
10
100
1000
retrieved
reference
initial guess
0.0
0.2
0.4
VMR [ppmv]
VMR retr - VMR ref [%]
total error [%]
χ^2 = 0.25
-40
-20
0
20
40
Percentage VMR errors [%]

Fig. 13

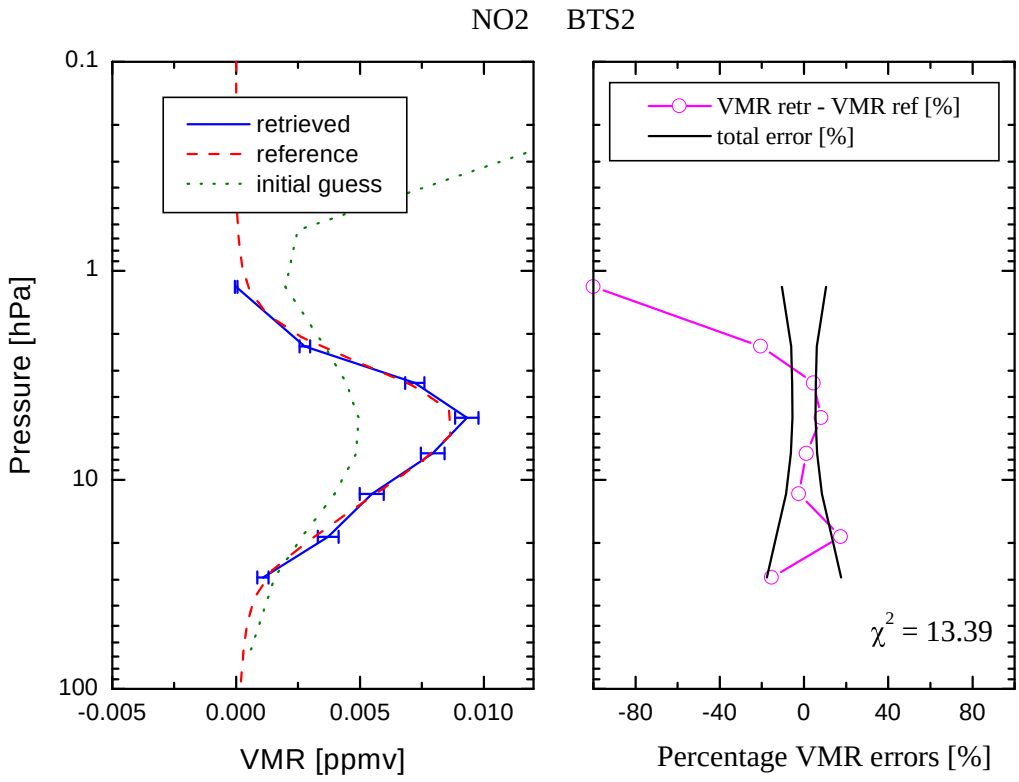
NO2 BTS2
Pressure [hPa]
0.1
1
10
100
retrieved
reference
initial guess
-0.005
0.000
0.005
0.010
VMR [ppmv]
VMR retr - VMR ref [%]
total error [%]
χ^2 = 13.39
-80
-40
0
40
80
Percentage VMR errors [%]

Fig. 14

3.1 Discussion of results

In general the observed discrepancies between retrieved and 'true' profiles are consistent with the estimated total error of the retrieved profiles. However there are a few exceptions to this general rule and in this section we analyze the origin of the relatively large discrepancies observed in these few cases.

In the retrieval algorithm the topmost and the lowermost retrieved profile points are used to scale the initial guess profiles outside the retrieval altitude range, so that the initial guess profile turns out to be smoothly connected with the retrieved profile at the edges of the retrieval range. This approach implies that if the assumed shape of the initial guess profile outside the retrieval range is different from the shape of the real profile, the topmost and the lowermost retrieved points are affected by an extra error due to the fact that the fit tries to compensate for the different shape of retrieved and initial guess profiles outside the retrieval range using the extreme retrieved points. So far the Oxford tool evaluating the total error budget does not account for this type error which, therefore, may show-up as an unpredicted discrepancy in our results. For this reason we also repeated the BTS2 retrievals using as initial guess the 'true' profiles perturbed using only scaling factors (in this case the shape of the initial guess was consistent with the shape of the 'true' profiles). We named "CS" this test (CS = Correct Shape). The CS test showed that this "shape error" affects significantly the BTS2 retrievals in the following cases:

1. Pressure at high altitudes (only marginally at low altitudes)
2. Temperature at high altitudes,
3. Water below the hygropause,
4. NO_2 at high altitudes

For these particular cases the results of the CS test are shown, in Fig's 7bis, 8bis, 9bis and 14bis respectively, using the same format as for the BTS tests shown before. The CS test shows also that the "shape error" is not an issue for ozone and nitric acid (results not shown here) that are the remaining two cases with relatively large discrepancies between "true" and retrieved profiles.

Comparison between results of BTS1 and BTS2 tests shows that at low altitudes tangent pressure error (that is ~ 9%) has a significant impact on both ozone and nitric acid retrievals at the same altitudes. The total error reported in the plots (calculated by the Oxford tool, MWMAKE) accounts only for a 3% pressure error. Most likely this large error in the retrieved pressure at low tangent altitudes in BTS2 is due to the large correlation existing between atmospheric continuum and tangent pressure at these altitudes.

The discrepancy observed in the retrieval of nitric acid at high altitude in the BTS1 test is the only case for which there is a relatively weak explanation: at this altitude the amount of HNO_3 is very little and the retrieval provides very unstable values for both VMR and its noise error. We think that the discrepancy observed at high altitudes in the HNO_3 BTS1 retrieval is smaller than that observed in the BTS2 case only because of a different number of iterations that took place in the two tests.

Methane and N_2O retrievals had no problems in all the analyzed test cases.

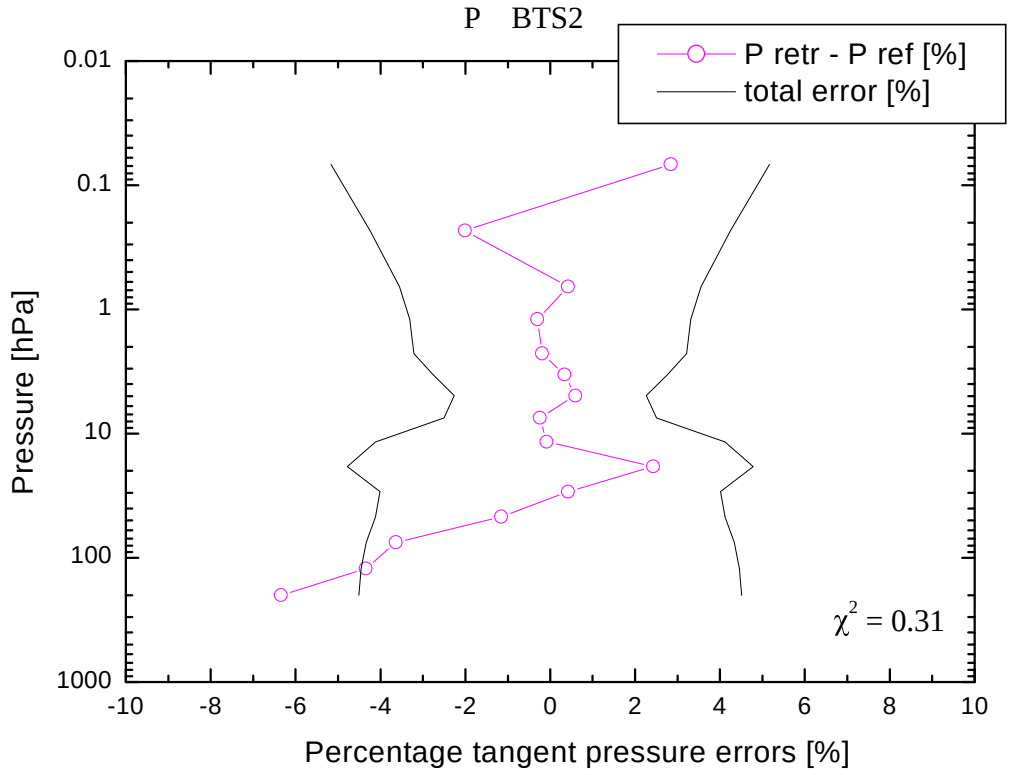

Fig. 7bis

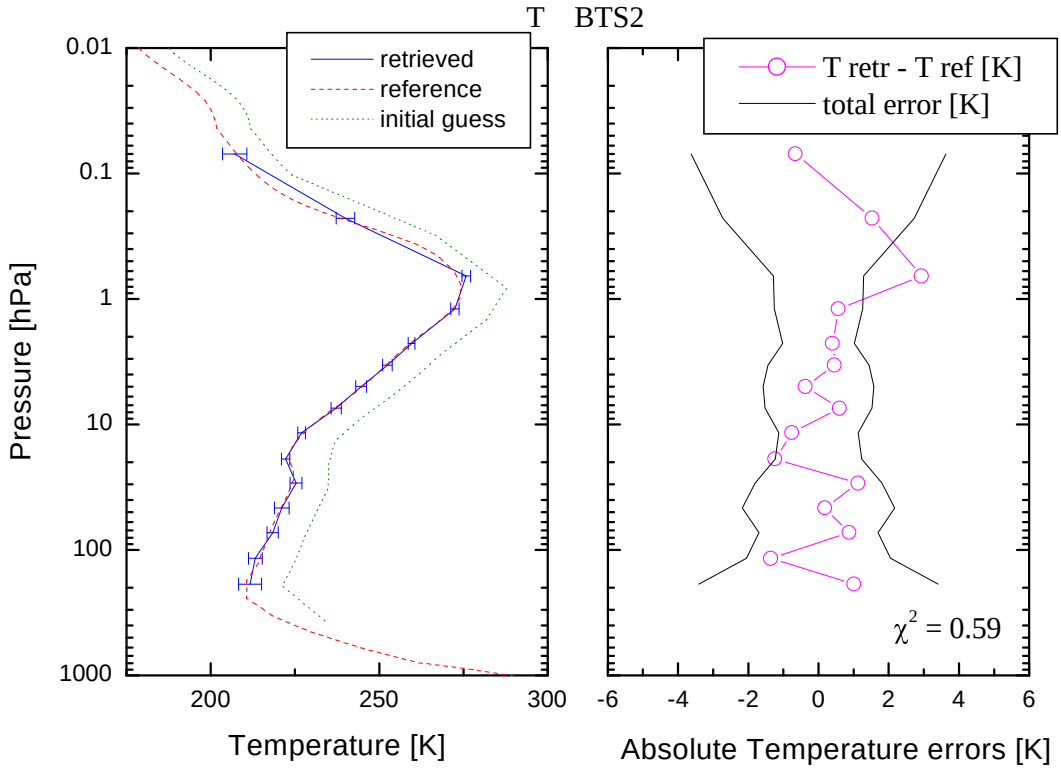

Fig. 8bis

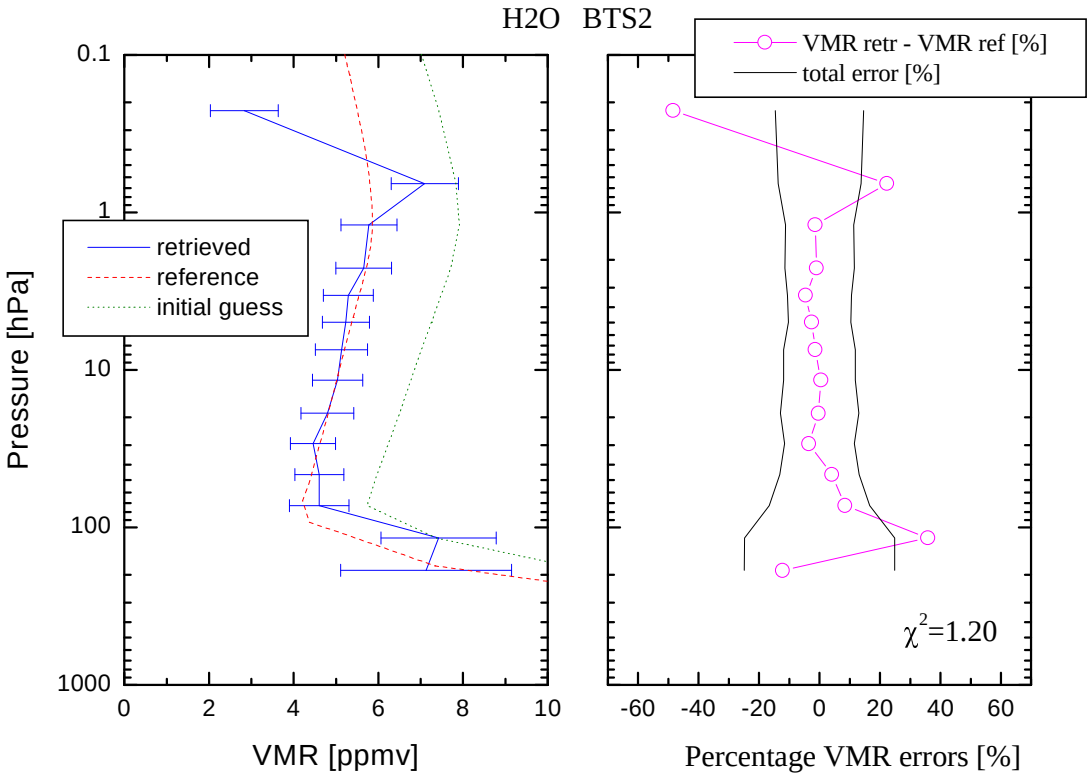

Fig. 9bis

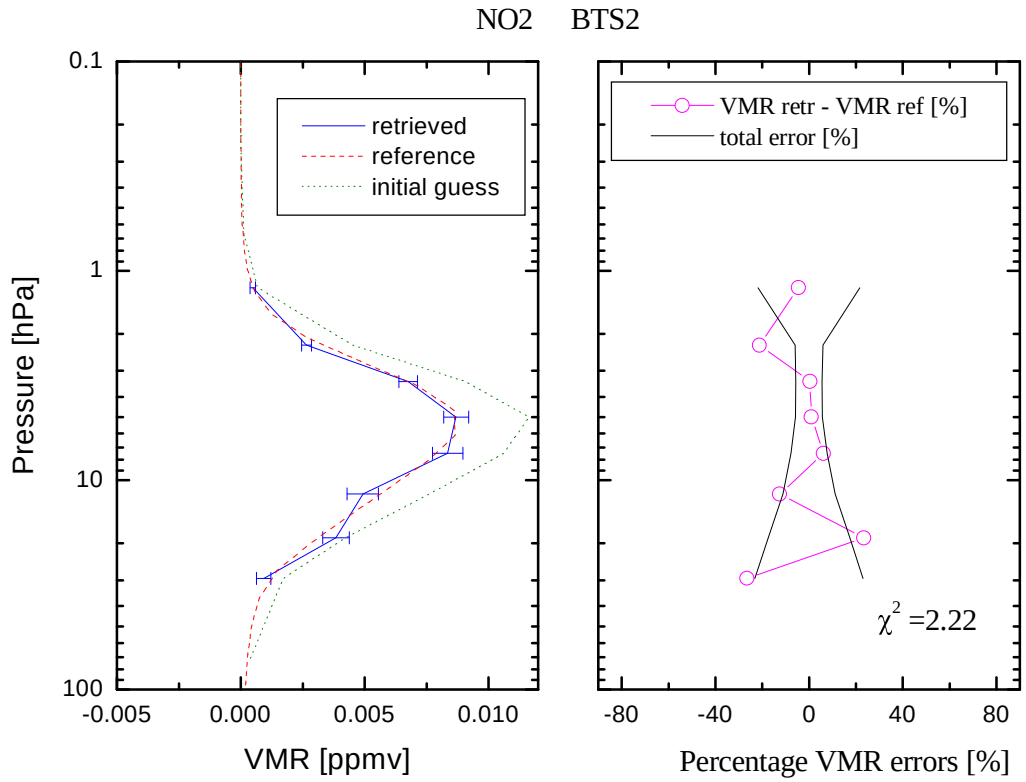

Fig. 14bis

3.2 Conclusions of blind test retrievals

Based on the results of blind test retrievals the following conclusions can be drawn:

1. In general the ORM_R provides stable results also in presence of systematic errors in the forward model. In particular, the following systematic error sources are active in our test retrievals:
   - VMR profiles of contaminants assumed in the ORM_R are different (within the limits of the atmospheric variability) compared to the profiles assumed by IAA for the generation of simulated observations,
   - ORM_R operates in LTE conditions while observations are simulated including NLTE
   - ORM_R neglects line-mixing while simulated observations include line-mixing
   - ORM_R neglects pressure shift and self-broadening while simulated observations do include these effects
   - "shape error" explained in Sect. 3.1.
2. The error estimates supplied by the Oxford tool (MWMAKE) and the VCM of the retrieval are in general consistent with the discrepancies between retrieved and reference (true) profiles with a good confidence level. The only discrepancies not fully consistent with the error predictions were found in the cases in which a) the "shape error" (presently neglected in MWMAKE, but will be included in a coming version) is significant and b) the tangent pressure error exceeds its expected value (3%).
3. Neglecting pressure-shift and self-broadening does not impact the accuracy of the retrieved profiles in the considered test cases. Therefore there is no clear indication suggesting that these two effects can not be neglected in MIPAS retrievals.
4. The loss of accuracy due to neglecting NLTE and Line-Mixing can be adequately controlled using an appropriate selection microwindows for the retrieval. Therefore, again, there is no clear indication suggesting that simulation of NLTE and Line-Mixing is compulsory for the retrieval of MIPAS key species at the accuracy level shown in Figs 1-14.

After these conclusions it was decided not to improve the ORM_R accuracy by including simulation of presently neglected effects, but rather to upgrade the retrieval code (named ORM_I) to include the capability of detecting in MIPAS spectra possible anomalies that may be due to residual effects for which a correction is operated in Level 1b processing (e.g. frequency and intensity calibration, ILS determination, instrumental offset).

4. New functionalities implemented in the ORM_I

The new functionalities introduced in the ORM_I are:

- Additional fit of ILS broadening parameter
- Additional fit of frequency scaling parameter
- Additional fit of intensity scaling parameter
- Fit of a MW- and altitude- dependent instrumental offset

4.1 Fit of a ILS broadening parameter

ILS broadening strongly affects tangent pressure and temperature retrieval, as well as VMR retrievals. The fit of an ILS broadening parameter can identify possible errors in the ILS function provided by Level 1b processor (see also *Stiller et al., (1995)*). The width of the ILS function can be changed by multiplying the ILS, in the interferogram domain, by a rectangular trapezium defined as follows:

$$\text{trapezium}(x) = (1-\alpha)\ \text{rectangle}_{\text{MPD}}(x) + \alpha\ \text{triangle}_{\text{MPD}}(x),$$

where:

$$\text{rectangle}_{\text{MPD}}(x) = \begin{cases} 1 & |x| \le \text{MPD} \\ 0 & |x| \ge \text{MPD} \end{cases}$$

$$\text{triangle}_{\text{MPD}}(x) = \begin{cases} 1 - x/MPD & |x| \le \text{MPD} \\ 0 & |x| \ge \text{MPD} \end{cases}$$

and MPD identifies the Maximum Path Difference.

The multiplying factor α, allowed to take values between -1 and 1, represents the ILS broadening parameter. The ILS broadening increases as α increases, a "sharpening" of the ILS occurs when $\alpha<0$. In the spectral domain the multiplication of the ILS function by the trapezium function becomes a convolution of the ILS function (in the spectral domain) with the following function:

$$Broad(\sigma) = \alpha\ \text{sinc}(2\pi\sigma\ \text{MPD}) + (1-\alpha)\ \text{sinc}^2(\pi\sigma\ \text{MPD}/2)$$

One ILS broadening parameter is fitted for each MIPAS spectral band.
When the fit of ILS broadening is active, the AILS (= Apodized ILS) relating to each microwindow is obtained by convoluting the AILS provided by Level 1b for each microwindow with the function *Broad (σ)* defined above. The derivatives of the spectrum with respect to the ILS broadening parameter of each band are calculated numerically, by convoluting the high resolution spectrum once with the broadened AILS function computed as described above, and once with a perturbed broadened AILS, obtained as the previous one but with a perturbed α parameter.
Since the result of convolution of a given finite vector **a** with a finite vector **b** is a vector whose length is (length_**a** - length_**b**), when the fit of ILS broadening is activated an extended AILS function is expected as input of the program (default AILS function length equal to 0.375 cm^{-1}).

4.2 Fit of a frequency shift parameter

Frequency calibration operated in Level 1b processor may not be perfect and, in this case, retrieval results are expected to improve if a frequency shift parameter is fitted.
A different frequency shift parameter for each MIPAS spectral band is fitted. A shift in the frequency calibration is applied as a modification of the AILS function of each microwindow. The AILS of each microwindow is obtained by convoluting the AILS provided by Level 1b with a "shifted" *sinc* function. The "shifted" *sinc* function is sampled at the MIPAS nominal resolution (0.025 cm^{-1}) but its zero position is shifted by a frequency step equal to the product of the central frequency of the microwindow times the frequency shift parameter (k) relating to the band to which the microwindow belongs.
As in the case of the fit of ILS broadening parameter, derivatives of the spectrum with respect to the frequency shift parameter of each band are computed numerically and when the fit of frequency shift is enabled, an extended AILS function is expected as input of the program. When the fit of frequency shift is enabled, the consistency of the length of the input AILS function is checked internally in the code.

4.3 Fit of intensity scaling parameter

An error in the intensity calibration of the spectra consists of a scaling factor applied to the spectrum. If the intensity calibration performed by Level 1b is not perfect (in particular different spectral bands may be characterized by different intensity calibration errors) the fit of the intensity calibration parameter provides an indication of the calibration errors.
Two fitting modes are foreseen: either only one parameter per band is fitted, or two parameters per band are fitted, one for the reverse sweeps and one for the forward sweeps.

4.3 Fit of a MW- and altitude- dependent instrumental offset

The ORM_R is able to fit only a MW- dependent and altitude- independent instrumental offset. In practice the instrumental offset could also depend on tangent altitude because the total radiance entering in the instrument depends on tangent altitude. We therefore implemented in the ORM_I the possibility of fitting an instrumental offset that is both altitude- and MW- dependent.
However, since some of the MWs used for the retrieval do not contain enough information to retrieve an altitude- dependent offset (in some cases the instrumental offset is highly correlated with the atmospheric continuum), in the ORM_I it is possible to select the MWs for which an altitude-dependent offset is fitted, for the other MWs (expected to contain not enough information to discriminate between offset and atmospheric continuum) only one offset parameter is fitted valid at all altitudes.

5. Test of the new functionalities of ORM

5.1 Fit of a ILS broadening parameter

Simultaneous fit of pT and ILS broadening parameters and simultaneous fit of water VMR and ILS broadening parameters have been tested. A different ILS broadening parameter (α) is fitted for each MIPAS spectral band.
The simulated observations used in these tests were generated by the OFM_R using a reference profile for pressure, temperature and VMR and $\alpha = 0$.
The initial guess for the retrievals are the followings:

- ILS broadening: $\alpha = 0.5$ in all MIPAS spectral bands
- Temperature: a perturbation of 5% with respect to the reference profile is added
- VMR: a perturbation of 35% with respect to the reference profile is added

The results of pT and water are shown in Figs. 15, 16 and 17. We report in the horizontal axis the differences between the retrieved profiles (together with the random errors) and the reference profiles, for temperature, pressure and H_2O VMR are shown as a function of the altitude (y axis). In the same figures the differences between the initial guess profiles and the reference profiles are shown too.

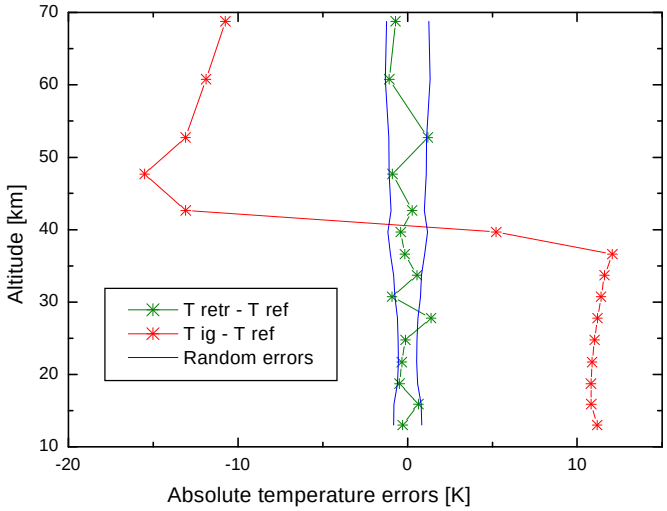

Fig. 15 Green line: absolute difference between the retrieved profile and the reference profile of temperature; red line: absolute difference between the initial guess profile and the reference profile of temperature; bleu: lines plus and minus one standard deviation of the error distribution on the retrieved temperature profile.

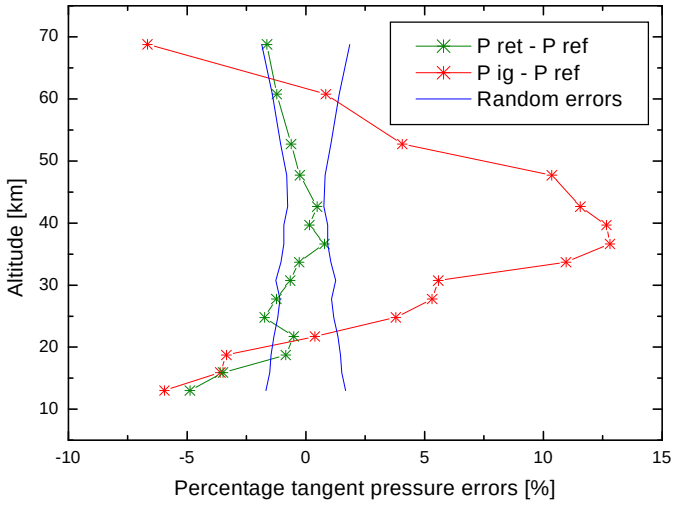

Fig. 16 Green line: percentage difference between the retrieved profile and the reference profile of pressure; red line: percentage difference between the initial guess profile and the reference profile of pressure; bleu lines: plus and minus one standard deviation of the error distribution on the retrieved pressure profile.

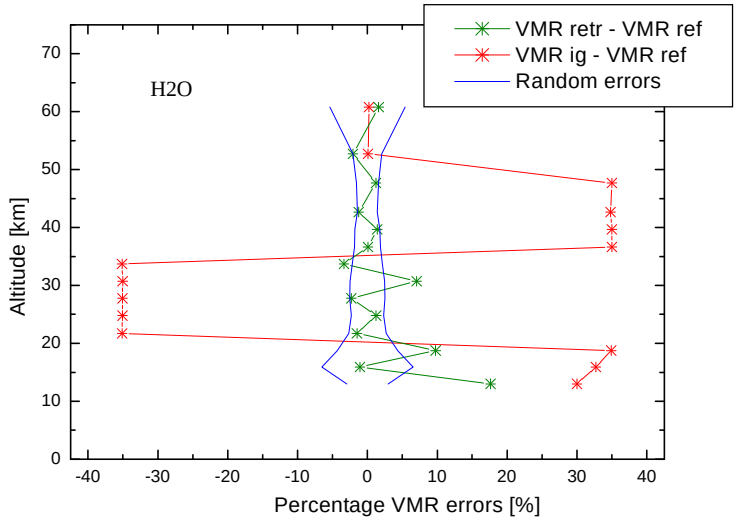

Fig. 17 Green line: percentage difference between the retrieved profile and the reference profile of water vapour; red line: percentage difference between the initial guess profile and the reference profile of water vapour; bleu lines: plus and minus one standard deviation of the error distribution on the retrieved water vapour profile.

In table 2 and 3 we show the retrieved values of the ILS broadening parameters:

Table 2: PT retrieval, χ^2 = 1.086	
MIPAS Spectral Band	**α**
A	$(- 9.4 \pm 0.5) * 10^{-4}$
B	$(2.3 \pm 2.6) * 10^{-2}$
D	$(-8.5 \pm 31) * 10^{-3}$

Table 2: retrieved values of the ILS broadening parameters with their errors as evaluated from the VCM of the retrieval. Case of pT retrieval.

Table 3: H_2O retrieval, χ^2 = 0.994	
MIPAS Spectral Band	**α**
A	$(3.0 \pm 1.8) * 10^{-2}$
B	$(6.5 \pm 12) * 10^{-3}$
C	$(7.1 \pm 6.7) * 10^{-3}$

Table 3: retrieved values of the ILS broadening parameters with their expected errors as derived from the retrieval VCM. Case of H_2O retrieval.

In fig. 18 and 19 the spectra calculated using the initial guess profiles and the retrieved profiles respectively are compared with the simulated observations.

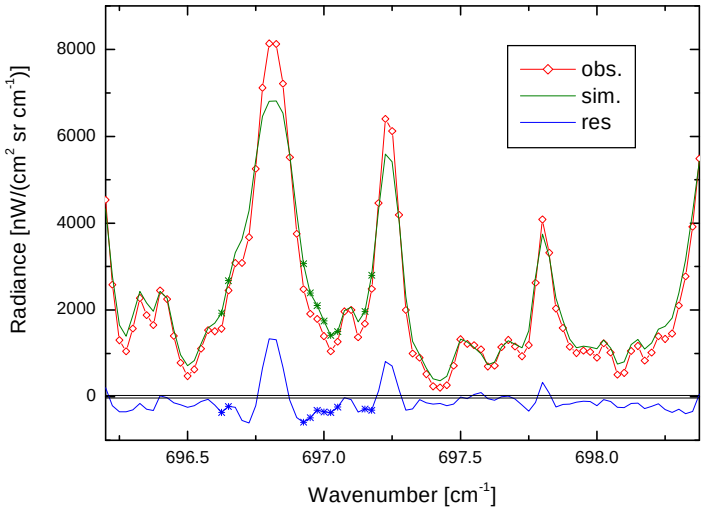

Fig. 18. Microwindow PT___oxf_017. Red lines with empty diamonds: simulated observations; green line: calculated spectrum using the initial guess profile; blue line: difference between red and green lines (residuals); black lines: plus and minus one standard deviation of the noise; green and blue asterisks: points used to perform the retrieval.

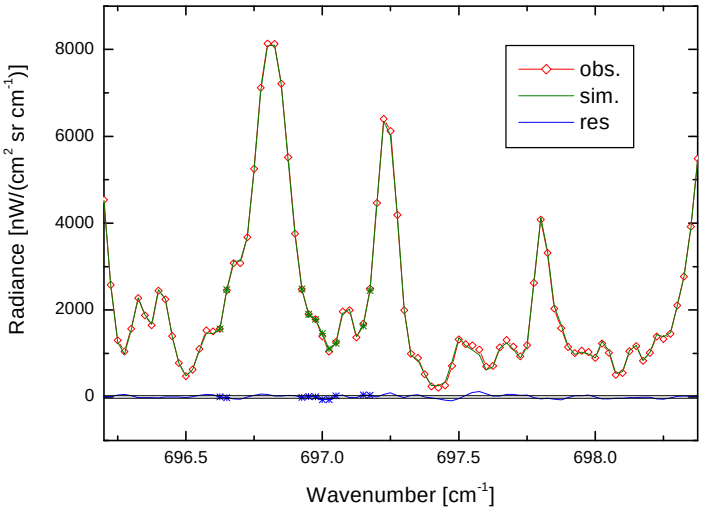

Fig. 19. Microwindow PT___oxf_017. Red lines with empty diamonds: simulated observations; green line: calculated spectrum using the retrieved profiles; blue line: difference between red and green lines (residuals); black lines: plus and minus one standard deviation of the noise; green and blue asterisks: points used to perform the retrieval.

The conclusion of this test is that simultaneous fits of ILS broadening parameters and pressure, temperature or VMR are feasible. It has been found that the thresholds used for convergence criteria are critical for these fits (meaning that conservative convergence criteria must be used).

5.2 Fit of frequency scaling parameter

Simultaneous fits of pressure, temperature or water vapour VMR and frequency scaling parameters have been performed. A different frequency scaling parameter (k) is fitted for each MIPAS spectral band.
The simulated observations employed in these retrievals were generated using the OFM_R with a reference profile for pressure, temperature and VMR and a k = 0.
The initial guess for the retrievals are the followings:

- Frequency scaling parameters: $k = 10^{-5}$ in all MIPAS spectral bands
- Temperature: a perturbation of 5% with respect to the reference profile is added
- VMR: a perturbation of 35% with respect to the reference profile is added

In figs. 20, 21 and 22 we report the results of the retrievals for temperature, pressure and water VMR. The horizontal axis is used to represent the differences between retrieved and reference profiles and the random error of the retrieved profiles. The vertical axis represents altitude. In the same figures the differences between the initial guess profiles and the reference profiles are shown as well.

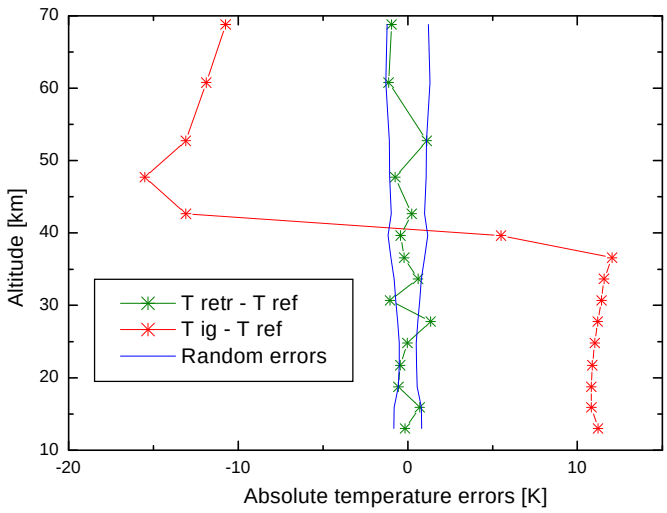

Fig. 20. Green line: absolute difference between the retrieved profile and the reference profile of temperature; red line: absolute difference between the initial guess profile and the reference profile of temperature; bleu lines: plus and minus one standard deviation of the error distribution on the retrieved temperature profile.

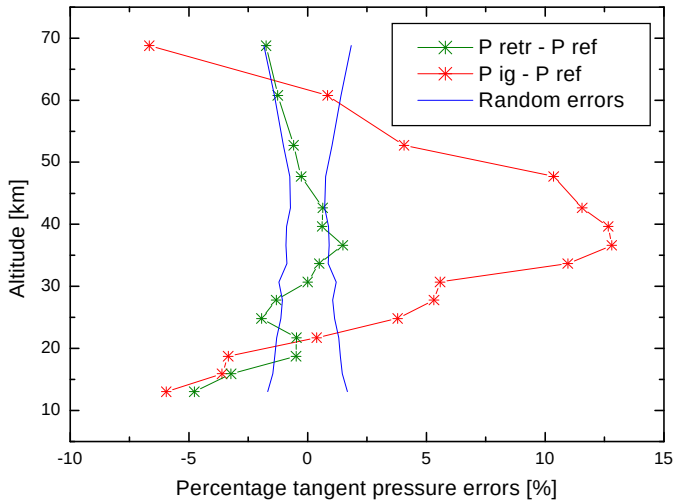

Fig. 21 Green line: percentage difference between the retrieved profile and the reference profile of pressure; red line: percentage difference between the initial guess profile and the reference profile of pressure; bleu lines: plus and minus one standard deviation of the error distribution on the retrieved pressure profile.

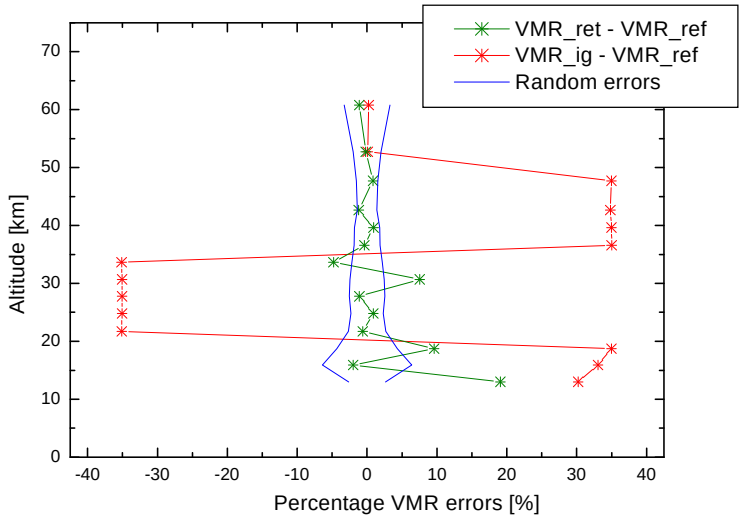

Fig. 22 Green line: percentage difference between the retrieved profile and the reference profile of water vapour; red line: percentage difference between the initial guess profile and the reference profile of water vapour; bleu lines: plus and minus one standard deviation of the error distribution on the retrieved water vapour profile.

In tables 4 and 5 the retrieved values of the frequency scaling parameters are shown:

Table 4: PT retrieval, $\chi^2 = 1.098$	
MIPAS Spectral Band	**k**
A	$(-6.6 \pm 72) * 10^{-9}$
B	$(-1.7 \pm 19) * 10^{-8}$
D	$(1.3 \pm 2.6) * 10^{-7}$

Table 4: retrieved values of the frequency scaling parameters with their expected standard deviations for PT retrieval.

Table 5: H_2O retrieval, $\chi^2 = 0.994$	
MIPAS Spectral Band	**k**
A	$(6.7 \pm 1.9) * 10^{-7}$
B	$(-1.2 \pm 1.1) * 10^{-7}$
C	$(-3.5 \pm 36) * 10^{-9}$

Table 5: retrieved values of the frequency shift parameters with their expected standard deviations for H_2O retrieval.

In fig. 23 and 24 the calculated spectra using the initial guess profiles and the retrieved profiles are compared with the simulated observations.

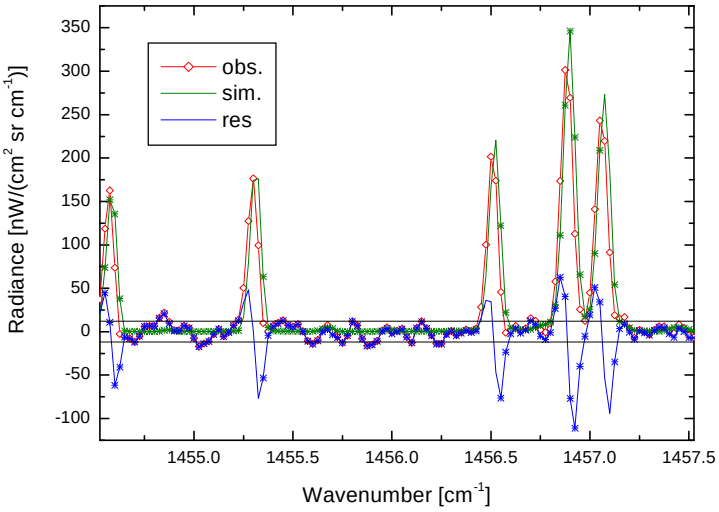

Fig. 23. Microwindow H2O___oxf_021. Red lines with empty diamonds: simulated observations; green line: calculated spectrum using the initial guess profile; blue line: difference between red and green lines (residuals); black lines: plus and minus one standard deviation of the noise; green and blue asterisks: points used to perform the retrieval.

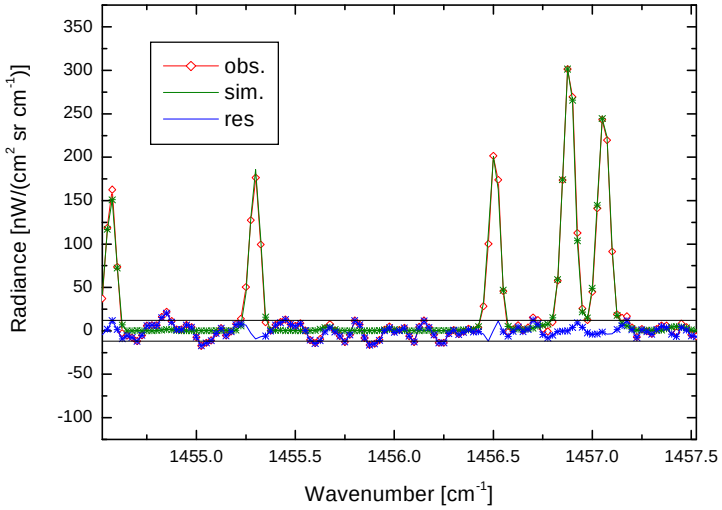

Fig. 24. Microwindow H2O___oxf_021. Red lines with empty diamonds: simulated observations; green line: calculated spectrum using the retrieved profiles; blue line: difference between red and green lines (residuals); black lines: plus and minus one standard deviation of the noise; green and blue asterisks: points used in the retrieval.

The conclusion of this test is that simultaneous fits of frequency shift parameters and pressure, temperature or VMR are feasible. From tables 4 and 5 we can see that the error associated to frequency shift parameters is of the order of $2*10^{-7}$. This precision is comparable with spectroscopic errors (which are sweep independent and transition dependent) and with Doppler shift due to wind (which is sweep dependent and band independent).

5.3 Fit of intensity scaling parameter

Simultaneous retrievals of pT or water VMR and intensity scaling parameters have been performed. A different frequency scaling parameter (*intcal*) is fitted for each MIPAS spectral band.
The simulated observations employed in these tests were generated using the OFM_R with a reference profile for pressure, temperature and VMR and *intcal* = 1.
The initial guess for the retrievals are the followings:

- Intensity calibration parameters: *intcal*(A band) = 1.2
  intcal(AB band) = 0.8
  intcal(B band) = 0.8
  intcal(C band) = 1.2
  intcal(D band) = 1.2
- Temperature: a perturbation of 5% with respect to the reference profile is added
- VMR: a perturbation of 35% with respect to the reference profile is added

In figs. 25, 26 and 27 the results of the retrievals for temperature, pressure and water vapour VMR are reported. In the horizontal axis the differences between the retrieved profiles (together with the random errors) and the reference profiles, for temperature, pressure and H2O VMR are shown as a function of the altitude (vertical axis). In the same figures the differences between the initial guess profiles and the reference profiles are shown too.

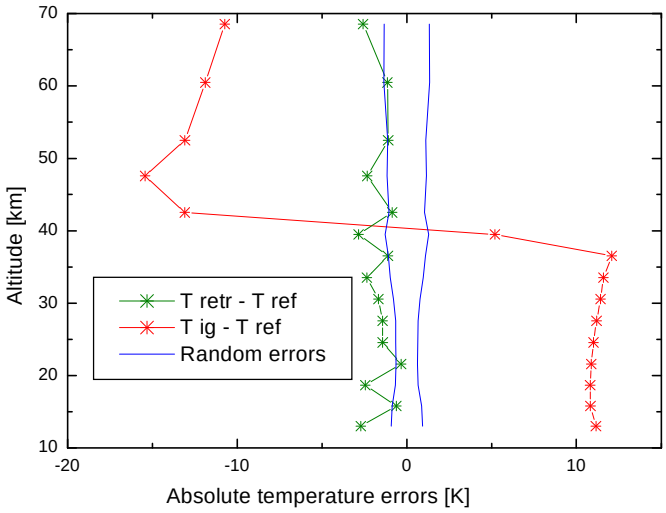

Fig. 25. Green line: absolute difference between the retrieved profile and the reference profile of temperature; red line: absolute difference between the initial guess profile and the reference profile of temperature; bleu lines: plus and minus one standard deviation of the error distribution on the retrieved temperature profile.

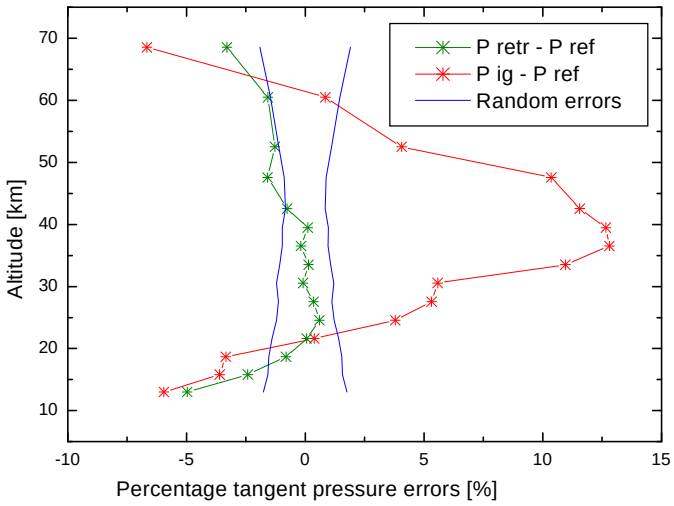

Fig. 26. Green line: percentage difference between the retrieved profile and the reference profile of pressure; red line: percentage difference between the initial guess profile and the reference profile of pressure; bleu lines: plus and minus one standard deviation of the error distribution on the retrieved pressure profile.

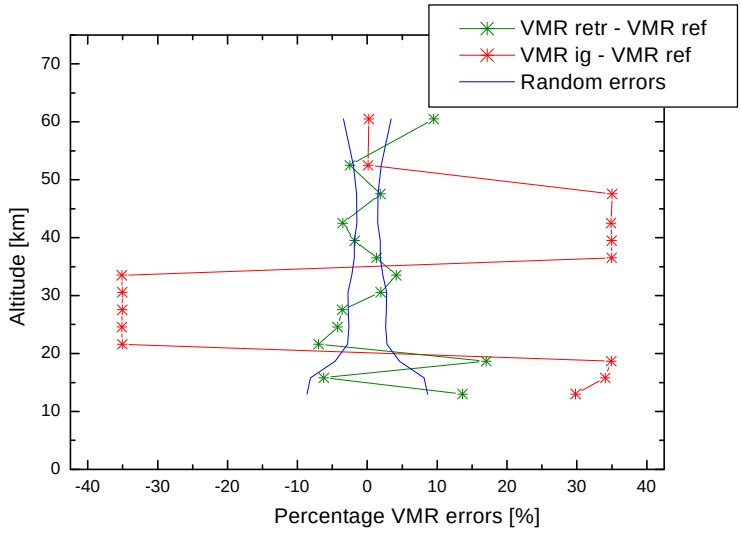

Fig. 27. Green line: percentage difference between the retrieved profile and the reference profile of water vapour; red line: percentage difference between the initial guess profile and the reference profile of water vapour; bleu lines: plus and minus one standard deviation of the error distribution on the retrieved water vapour profile.

In tables 6 and 7 we show the retrieved values of the intensity scaling parameters.

Table 6: PT retrieval, χ^2 = 1.107	
MIPAS Spectral Band	***Intcal***
A	1.033 ± 0.008
B	1.059 ± 0.015
D	1.065 ± 0.026

Table 6: retrieved values of the intensity scaling parameters with their expected standard deviations for PT retrieval.

Table 7: H_2O retrieval, χ^2 = 0.994	
MIPAS Spectral Band	***Intcal***
A	1.08 ± 0.09
B	1.069 ± 0.005
C	1.062 ± 0.003

Table 7: retrieved values of the intensity shift parameters with their expected standard deviations for H2O retrieval.

In figs. 28 and 29 the spectra simulated using the initial guess profiles and the retrieved profiles are compared with the simulated observations.

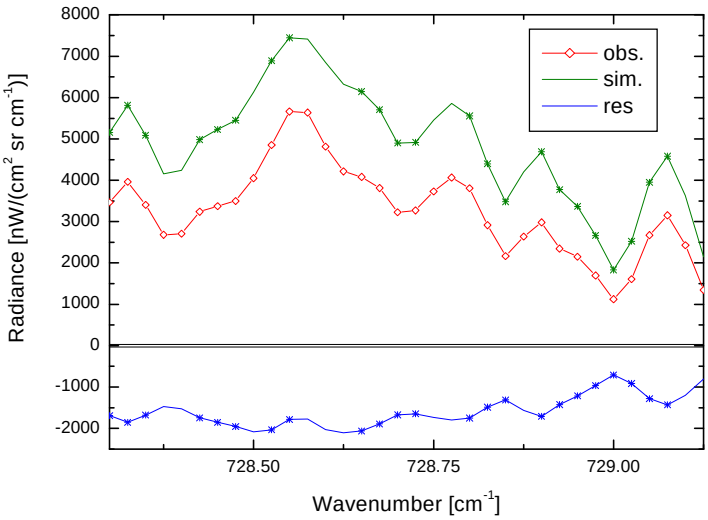

Fig. 28. Microwindow PT___oxf_004. Red lines with empty diamonds: simulated observations; green line: calculated spectrum using the initial guess profile; blue line: difference between red and green lines (residuals); black lines: plus and minus one standard deviation of the noise; green and blue asterisks: points used to perform the retrieval.

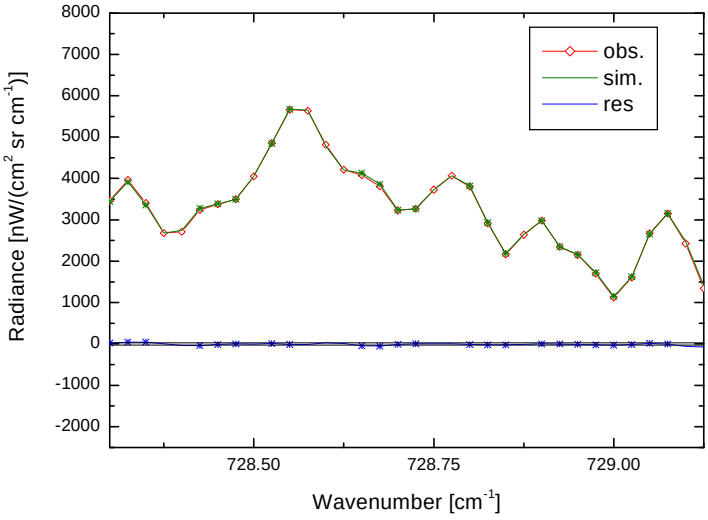

Fig. 29. Microwindow PT___oxf_004. Red lines with empty diamonds: simulated observations; green line: calculated spectrum using the retrieved profiles; blue line: difference between red and green lines (residuals); black lines: plus and minus one standard deviation of the noise; green and blue asterisks: points used to perform the retrieval.

From the results of this test we can see that there is a strong correlation between the intensity calibration parameters and temperature. An error of about 5% in the intensity calibration parameters determines an offset of about 2 K in the temperature profile. So it is not possible to determine the

absolute values of the intensity calibration parameters, but in case that microwindows belonging to different bands are used in the fit, the ratio between the intensity calibration parameters of different bands can be determined.

5.4 Fit of a MW- and altitude- dependent instrumental offset

Using the JUL01 MWs pT and H2O retrievals were attempted jointly with a MW- and altitude-dependent instrumental offset retrieval. We found that it is actually possible to retrieve a MW- and altitude- dependent instrumental offset jointly with pT or water VMR, however even if the retrieval is able to recover the reference altitude-dependent zero-level calibration within the ESD relating to these parameters, the ESD level itself exceeds in several cases the measurement noise. We conclude therefore that building of a precise statistics on the behaviour of the instrumental offset will be hardly feasible, at least with the JUL01 microwindows.

6. General conclusions

The blind test retrievals carried-out under the AMIL2DA study provided satisfactory results in terms of consistency of the observed discrepancies (retrieved minus "true" profiles) with the estimated total retrieval error. We therefore decided not to improve the ORM_R accuracy by including simulation of presently neglected effects, but rather to upgrade the retrieval code (named ORM_I) to include the capability of detecting in MIPAS spectra possible anomalies that may be due to residual effects for which a correction is operated in Level 1b processing (e.g. frequency and intensity calibration, ILS determination, instrumental offset).
The simultaneous retrieval of pT (or water) and an additional instrument- related parameter was found to be feasible and, in most cases provides results useful for the characterization of the instrument and Level 1b products performance.

7. References

- Bennett V., A.Dudhia, C.D.Rodgers, "Microwindow Selection for MIPAS Using Information Content", pp. 265-269 in proceedings of the European Symposium on Atmospheric Measurements from Space, 18-22 January 1999, ESTEC Noordwijk, The Netherlands
- Dudhia A., "A multi-layer technique for microwindow selection" PO-TN_OXF-GS-0013, delivery of the ESA contract 11886/96/NL/GS, CCN4, (21 September 1999)
- Ridolfi M., B.Carli, M.Carlotti, T.v.Clarmann, B.M.Dinelli, A.Dudhia, J.-M.Flaud, M.Hoepfner, P.E.Morris, P.Raspollini, G.Stiller, R.J.Wells, 'Optimized forward model and retrieval scheme for MIPAS near-real-time data processing' *Appl. Optics*, Vol. **39**, No. 8, p. 1323 – 1340 (10 March 2000)
- Stiller, G.P., T.v.Clarmann, A.Wegner, M.Baumann, E.Frank, H.Oelhaf, "Retrieval of Tropospheric Versus Stratospheric Partitioning of HCl from Ground--Based MIPAS FTIR Spectra", *J. Quant. Spectrosc. Radiat. Transfer*, Vol. **54**, No. 5, pp. 899-912, (1995)